

TeV Scale Resonant Leptogenesis with triplet Fermion in Connection to Muon $g - 2$

Simran Arora ^{*1}, Devabrat Mahanta ^{†2} and B. C. Chauhan ^{‡3}

^{1,3}*Department of Physics and Astronomical Science, Central University of Himachal Pradesh, Dharamshala 176215, INDIA.*

²*Department of Physics, Pragjyotish College, Gwahati 781009, INDIA*

Abstract

We propose an extension of the minimal scotogenic model with a triplet fermion and a singlet scalar. An imposed $Z_4 \times Z_2$ symmetry allows only diagonal Yukawa couplings among different generations of SM leptons and right-handed singlet neutrinos. The Yukawa coupling of the triplet fermion with the inert doublet positively contributes to the muon anomalous magnetic moment. The imposed $Z_4 \times Z_2$ symmetry forbids the conventional leptogenesis from the lightest right-handed neutrino decay. A net lepton asymmetry can be generated in the muonic sector from N_2 and triplet fermion decay through resonant leptogenesis scenario. The Yukawa coupling of triplet plays significant role both in leptogenesis and in the anomalous magnetic moment of the muon. We show a viable parameter space for TeV scale leptogenesis while explaining the Fermi lab results. The inert scalar is the dark matter candidate in this model. The Muon ($g - 2$) and dark matter both favor the same parameter space for mass of the dark matter and the triplet fermion.

Keywords: Z_4 symmetry, Muon ($g - 2$), Fermion triplet, Leptogenesis, Scalar Dark Matter.

*009simranarora@gmail.com

†devabrat@pragjyotishcollege.ac.in

‡bcawake@hpcu.ac.in

1 Introduction

Only $\sim 5\%$ of our Universe is made up of baryonic matter. The baryonic matter has a large asymmetry between the particles and antiparticles. This asymmetry is termed as the Baryon asymmetry of the Universe (BAU). The observed (BAU) is often quantified in terms of the baryon-photon ratio defined as [1]

$$\eta_B = \frac{n_B - n_{\bar{B}}}{n_\gamma} \simeq 6.2 \times 10^{-10}. \quad (1)$$

While the measured value of the baryon to photon ratio from the cosmic microwave background (CMB) measurement agrees with the big bang nucleosynthesis (BBN) estimate, the origin of baryon asymmetry has been a long-standing problem in particle physics and cosmology. To dynamically generate the required baryon asymmetry, three conditions were given by Sakharov [2] called "Sakharov Conditions" as (1) Baryon Number Violation, (2) C and CP violation and (3) out of equilibrium dynamics. All these requirements can be satisfied within the Standard Model (SM) with an expanding Universe. However, the required amount of asymmetry can not be generated within the SM. Therefore, it demands new physics beyond the SM. Among different baryogenesis mechanisms, leptogenesis is one of the most promising mechanisms as it connects the high scale baryogenesis to the low-scale neutrino oscillation data (For a few reviews on leptogenesis see [3–5] and the references therein). In a conventional leptogenesis scenario, the decay of heavy right-handed neutrinos into SM lepton doublets and SM Higgs accounts for small lepton asymmetry of the Universe, which later gets converted into baryon asymmetry through *sphaleron* process [6]. This mechanism is called Vanilla leptogenesis [7, 8]. In the conventional method, with two right-handed neutrinos, the mass of right-handed neutrinos is high ($M_1 \gtrsim 10^9$) GeV. Such high-mass right-handed neutrinos are difficult to probe in collider experiments. This motivates us to search for low-scale leptogenesis scenarios. In the minimal scotogenic model it is possible to have successful leptogenesis around the TeV scale [9] with three right-handed neutrinos. Although this is a minimal scenario to have low-scale leptogenesis, it is difficult to bring a connection with the observed excess in Muon ($g - 2$) measurement by the Fermi Lab. Another possible way to lower the scale of leptogenesis is resonant leptogenesis (RL), [10, 11] where the self-energy effects enhance the lepton asymmetry due to tiny mass splitting between two fermion states. This is achieved when the mass difference between these states is comparable to their decay widths. It allows for successful leptogenesis at TeV scale. See [9, 12–17] and references therein for a few low-scale leptogenesis models. Here we consider a leptogenesis scenario where a triplet fermion resonantly enhances the $B - L_\mu$ asymmetry that is also responsible for generating Muon ($g - 2$) excess.

Apart from the BAU, the existence of non-luminous dark matter (DM), giving a total contribution of around 26% of the present Universe's energy density has been an unsolved puzzle in cosmology and particle physics. The DM energy density is expressed in the density parameter Ω_{DM} . The Planck 2018 [1] data has reported the value for the DM density parameter at 68% CL

$$\Omega_{\text{DM}} h^2 = 0.120 \pm 0.001. \quad (2)$$

Here $h = \text{Hubble parameter}/(100 \text{ Km s}^{-1} \text{ Mpc}^{-1})$. While none of the Standard Model particles satisfy the conditions to be a DM candidate, the SM also fails to adequately explain the origin of the baryon asymmetry. Another important problem the SM fails to explain is the existence of non-zero neutrino masses. It has led to a number of extensions of the SM. There have been multiple attempts where it is successfully addressed along with the BAU and DM production (For a detailed review of such ideas see [18] and the references therein). The recent measurement by the Muon ($g - 2$) collaboration at Fermilab has reported a significant deviation in the anomalous magnetic moment $a_\mu = (g_\mu - 2)/2$ of the muon from the standard model prediction [19]. Upon combining Fermi lab results on Muon ($g - 2$) with the previous measurement from the Brookhaven National Laboratory shows a 4.2σ observed excess of $\Delta a_\mu = 251(59) \times 10^{-11}$. This result has led to different BSM proposals (a comprehensive review can be found in [20]). The authors of [14, 21, 22] have shown few possible connections between the Fermi lab results on Muon ($g - 2$) and the BAU. On the other hand, the authors of [23–27] had discussed few possible connections between DM and the Muon ($g - 2$) excess. To the authors’ knowledge, there have been no attempts to find a unified solution connecting both BAU and DM to the Muon ($g - 2$) excess.

In this work, we propose a minimal extension of the SM that can potentially address these key problems. We extend the minimal scotogenic model with a Majorana fermion triplet by using a discrete Z_4 symmetry that only allows diagonal Yukawa matrices. The neutrino mass is generated through the scotogenic mechanism in the model. The decay of N_2 and fermion triplet with an almost degenerate mass around the TeV scale leads to net lepton asymmetry in the muon sector due to imposed $Z_4 \times Z_2$ symmetry. The fermion triplet also has its role in explaining Muon ($g - 2$) through its coupling with inert doublet which is the dark matter candidate in the model.

The rest of the paper is organized as follows: In Section 2, we briefly discuss our basic framework and the corresponding Lagrangian. Section 2.1 provides a detailed description of the neutrino mass mechanism through the scotogenic model. In Section 2.2, we introduce the Muon ($g - 2$) and the results for the proposed model, in Section 2.3, we provide the analysis of inert dark matter in the model. In section 2.4, low-scale leptogenesis by out of equilibrium decay of the right-handed neutrino N_2 assisted by fermion triplet is explained. Section 2.4.1 presents the detailed summary of the results from the model. In Section 3, we have concluded the work.

2 The Model

The scotogenic neutrino mass generation proposed in [28] has been a very promising minimal extension of the SM explaining the origin of non-zero neutrino mass. The scotogenic model not only provides an elegant way of DM production but also can generate the observed baryon asymmetry at relatively low scales. The authors [9] have shown the possibility of a TeV scale leptogenesis in the minimal scotogenic model. A few different leptogenesis scenarios in the context of the scotogenic model can be found in [15, 29, 30]. In this paper, we propose extending the scotogenic model with a triplet fermion. The particle content of the model is shown in table (1). The SM is extended by three copies of right-handed neutrinos (N_i), a

triplet fermion (ψ), a scalar singlet (S) and an inert doublet (η). All the fields are charged under an imposed $Z_4 \times Z_2$ symmetry as shown in the table (1).

Symmetry Group	L_e, L_μ, L_τ	e_R, μ_R, τ_R	N_1, N_2, N_3	ψ	H	S	η
$SU(2)_L \times U(1)_Y$	(2, -1/2)	(1, -1)	(1, 0)	(3, -1)	(2, 1/2)	(1, 0)	(2, 1/2)
Z_4	(1, $i, -i$)	(1, $i, -i$)	(1, $i, -i$)	i	1	$-i$	1
Z_2	+	+	-	-	+	+	-

Table 1: The field content and respective charge assignments of the model under $SU(2)_L \times U(1)_Y \times Z_4 \times Z_2$.

The relevant terms in the Yukawa Lagrangian are

$$\begin{aligned}
-\mathcal{L} \supseteq & \frac{M_{11}}{2} N_1 N_1 + M_{23} N_2 N_3 + y_{\eta 1} \bar{L}_e \tilde{\eta} N_1 + y_{\eta 2} \bar{L}_\mu \tilde{\eta} N_2 + y_{\eta 3} \bar{L}_\tau \tilde{\eta} N_3 \\
& + y_{12} S N_1 N_2 + y_{13} S^* N_1 N_3 + y_\psi \bar{L}_\mu C \psi^\dagger \tilde{\eta} + m_\psi \bar{\psi}(\psi)^c \\
& + y_e \bar{L}_e H e_R + y_\mu \bar{L}_\mu H \mu_R + y_\tau \bar{L}_\tau H \tau_R + H.c.,
\end{aligned} \tag{3}$$

with $\tilde{\eta} = i\sigma_2 \eta^*$ and the scalar potential $V(H, S, \eta)$ is given by

$$\begin{aligned}
V(H, S, \eta) = & -\mu_H^2 (H^\dagger H) + \lambda_1 (H^\dagger H)^2 - \mu_S^2 (S^\dagger S) + \lambda_S (S^\dagger S)^2 + \lambda_{HS} (H^\dagger H)(S^\dagger S) \\
& + \mu_\eta^2 (\eta^\dagger \eta) + \lambda_2 (\eta^\dagger \eta)^2 + \lambda_3 (\eta^\dagger \eta)(H^\dagger H) + \lambda_4 (\eta^\dagger H)(H^\dagger \eta) \\
& + \frac{\lambda_5}{2} [(H^\dagger \eta)^2 + (\eta^\dagger H)^2] + \lambda_{\eta S} (\eta^\dagger \eta)(S^\dagger S) + H.c..
\end{aligned} \tag{4}$$

The SM gauge symmetry is broken by the neutral component of Higgs doublet H while the Z_4 symmetry is spontaneously broken by the non-zero vacuum expectation value (VEV) of scalar singlet S . Also, we assume $\mu_\eta^2 > 0$ so that η do not acquire any VEV. Hence the masses of singlet scalar and Higgs are given as

$$m_{S,H}^2 = \lambda_1 v^2 + \lambda_S v_S^2 \pm (\lambda_1 v^2 + \lambda_S v_S^2) \sqrt{1 + r^2}, \tag{5}$$

where $r = \frac{\lambda_{HS} v v_S}{\lambda_1 v^2 - \lambda_S v_S^2}$. The masses of neutral and charged components of inert doublet are written as

$$m_{\eta^\pm}^2 = \mu_\eta^2 + \frac{1}{2} \lambda_3 v^2 + \frac{1}{2} \lambda_{\eta S} v_S^2, \tag{6}$$

$$m_{\eta_R}^2 = \mu_\eta^2 + \frac{1}{2} \lambda_3 v^2 + \frac{1}{2} (\lambda_4 + \lambda_5) v^2 + \frac{1}{2} \lambda_{\eta S} v_S^2, \tag{7}$$

$$m_{\eta_I}^2 = \mu_\eta^2 + \frac{1}{2} \lambda_3 v^2 + \frac{1}{2} (\lambda_4 - \lambda_5) v^2 + \frac{1}{2} \lambda_{\eta S} v_S^2. \tag{8}$$

Here it is important to note that $m_{\eta_R}^2 - m_{\eta_I}^2 = \lambda_5 v^2$. Using Eq. (3), the charged lepton mass matrix M_l , Dirac Yukawa matrix y_D and right-handed neutrino mass matrix M_R are given by

$$M_l = \frac{1}{\sqrt{2}} \begin{pmatrix} y_\epsilon v & 0 & 0 \\ 0 & y_\mu v & 0 \\ 0 & 0 & y_\tau v \end{pmatrix},$$

$$y_D = \begin{pmatrix} y_{\eta 1} & 0 & 0 \\ 0 & y_{\eta 2} & 0 \\ 0 & 0 & y_{\eta 3} \end{pmatrix}, M_R = \begin{pmatrix} M_{11} & y_{12} v_S / \sqrt{2} & y_{13} v_S / \sqrt{2} \\ y_{12} v_S / \sqrt{2} & 0 & M_{23} e^{i\delta} \\ y_{13} v_S / \sqrt{2} & M_{23} e^{i\delta} & 0 \end{pmatrix}. \quad (9)$$

Here $v/\sqrt{2}$ and $v_S/\sqrt{2}$ are *vevs* of the Higgs field H and scalar field S , respectively, and δ is the phase remaining after redefinition of the fields.

2.1 Neutrino Mass

In this model, neutrinos get mass by the scotogenic mechanism [28]. The light neutrino mass matrix is given by

$$M_{ij}^\nu = \sum_{k=1}^3 \frac{d_{ik} d_{jk} M_k}{32\pi^2} [L_k(m_{\eta_R}^2) - L_k(m_{\eta_I}^2)], \quad (10)$$

where

$$L_k(m^2) = \frac{m^2}{m^2 - M_k^2} \ln \frac{m^2}{M_k^2}. \quad (11)$$

Here M_k is the mass of k^{th} right-handed neutrino and m_{η_R, η_I} are the masses of real and imaginary parts of inert doublet η and indices $i, j = 1, 2, 3$ run over three neutrino generations. Here $d_{ik} = y_{\eta i} C_{ik}$, where C_{ik} are the elements of the matrix that diagonalize M_R . We use the Casas-Ibarra (CI) [31] parametrization for radiative seesaw mechanism [32] through which the Yukawa coupling satisfy neutrino oscillation data. The parametrization is given by

$$d_{ik} = (UD_\nu^{1/2} R^\dagger \Lambda^{1/2})_{ik}. \quad (12)$$

Here R is a complex orthogonal matrix, $D_\nu = \text{diag}(m_1, m_2, m_3)$ is diagonal light neutrino mass matrix. The entries of the diagonal matrix Λ is given by

$$\Lambda_k = \frac{2\pi^2}{\lambda_5} \zeta_k \frac{2M_k}{v^2}, \quad (13)$$

where

$$\zeta_k = \left(\frac{M_k^2}{8(m_{\eta_R}^2 - m_{\eta_I}^2)} [L_k(m_{\eta_R}^2) - L_k(m_{\eta_I}^2)] \right). \quad (14)$$

2.2 Muon ($g - 2$)

The fermion triplet ψ explains Muon ($g - 2$) by its coupling with SM muon and inert doublet η . The Feynman diagrams for the same are given in Fig. (1). The additional contribution to Muon ($g - 2$) is given as [33]

$$\Delta a_\mu = \frac{m_\mu^2 y_\psi^2}{32\pi^2 m_\eta^2} [5f_1(m_\psi^2/m_\eta^2) - 2f_2(m_\psi^2/m_\eta^2)], \quad (15)$$

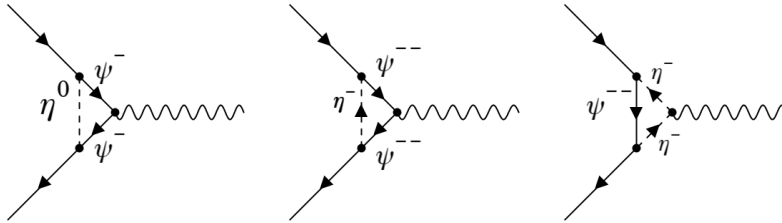


Figure 1: Feynman diagrams showing the contribution of fermion triplet to Muon ($g - 2$).

where m_μ , m_ψ , m_η are the masses of muon, fermion triplet ψ , inert scalar doublet η respectively. Here we keep the masses of the neutral scalars (η_R, η_I) and the charged scalars (η^\pm) nearly the same and are represented by m_η . The loop functions are given by

$$f_1(x) = \frac{1}{6(x-1)^4} [x^3 - 6x^2 + 3x + 2 + 6x \ln x],$$

$$f_2(x) = \frac{1}{6(x-1)^4} [-2x^3 - 3x^2 + 6x - 1 + 6x^2 \ln x]. \quad (16)$$

Here, x is a dimensionless parameter given by $x = m_\psi^2/m_\eta^2$. In Fig. (2) we show the data points that satisfy the Fermi lab result on Δa_μ . In the left panel plot, we show the data points within the allowed range of Δa_μ from the Fermi Lab result on Muon $g - 2$ with m_ψ in the x-axis and y_ψ as color bar. In the right panel plot, we show the allowed parameter space from the Fermi Lab result on Muon ($g - 2$) in $m_\eta - \Delta m$ plane, $\Delta m = m_\psi - m_\eta$ being the mass difference between the triplet fermion ψ and the doublet scalar η . The Yukawa coupling y_ψ is shown by the color bar. From the right panel plot of Fig. (2) it can be seen that to satisfy the Fermi lab results on Muon ($g - 2$) excess one need $m_\eta \simeq m_\psi$. With $m_\eta \simeq m_\psi$ the contribution to Muon ($g - 2$) coming from the diagrams shown in Fig. (1) enhances. To produce the observed excess of Muon ($g - 2$) we require the $m_\eta \simeq m_\psi$ even with the maximum possible value of $y_\psi = 4\pi$. Here we take the Yukawa coupling in the range $0.001 \leq y_\psi \leq 1$. From the left panel plot in Fig. (2), it can be seen that there exists a correlation between m_ψ and y_ψ . With the increase in m_ψ we require lower values of y_ψ to generate the observed Muon $g - 2$ excess. Similarly from the right panel plot in Fig. (2) one can notice a positive correlation between the Δm and y_η . With the increase in Δm , the required value of y_ψ increases. Also it is seen that there is a negative correlation between m_η and y_ψ .

2.3 Dark Matter

In the minimal scotogenic model, scalar and fermionic DM scenarios are possible depending on the lightest Z_2 odd state. The lightest of the neutral components of the inert doublet η serves to be a weakly interacting massive particle (WIMP) DM. This scenario is extensively studied in the literature [30, 34, 35]. If the inert doublet scalar becomes heavier than the lightest right-handed neutrino, the latter becomes a DM candidate. Depending on the size of Yukawa couplings, the fermionic DM can be produced thermally or non-thermally [30]. Here, we take the scalar DM scenario, where the real part of the neutral component of

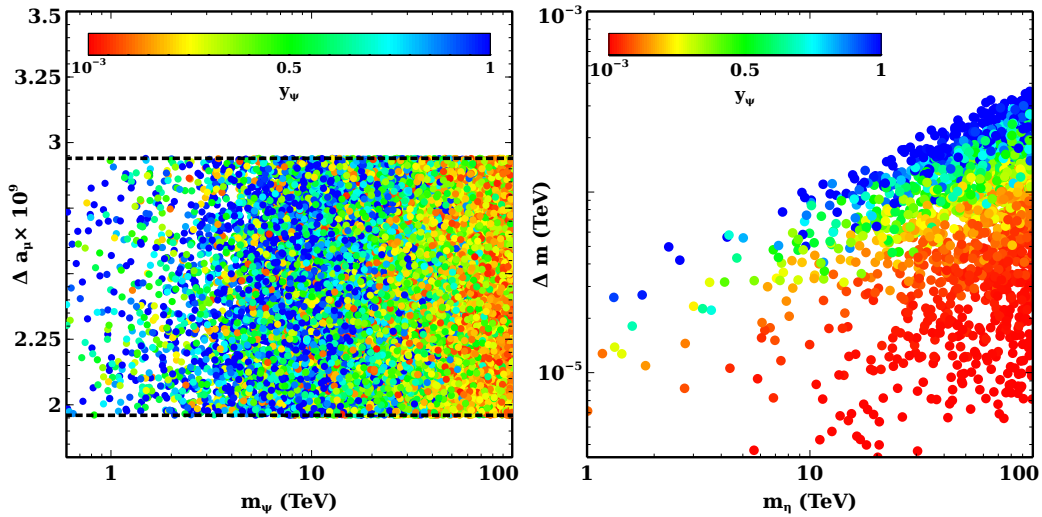


Figure 2: Plots showing the data points allowed by the Fermi lab’s result on Muon ($g - 2$). Right panel shows the parameter space in $m_\eta - \Delta m$ plane with y_ψ as the color bar and the left panel shows the allowed data points with m_ψ and $\Delta a_\mu = 251(59) \times 10^{-11}$. Here m_ψ is varied randomly from 0.75 TeV to 100 TeV and $m_\eta = m_\psi - \Delta m$, with Δm varied from 10^{-6} TeV to 10^{-3} TeV.

the inert doublet is the DM particle. The model is implemented in Feynrules [36, 37] to compute all the relevant vertices. To solve the Boltzmann equations and to calculate the relic density of dark matter, micrOMEGAs is used [38, 39]. Apart from the annihilation and co-annihilation of inert doublet DM, here we also have a few additional co-annihilation of the DM with the triplet fermion ψ . The co-annihilation processes are shown in Fig. (3). The relevant cross-sections for the co-annihilation processes are shown in Appendix A.

To satisfy the correct relic, the parameter space is constrained in $m_\psi - y_\psi$ plane which is relevant for leptogenesis and Muon ($g - 2$) as well. On the top left panel plot of Fig.(4), we show the parameter space allowed by the correct DM relic in $m_\eta - \Delta m$ plane. Since the mass required for the doublet scalar to satisfy the Fermi lab result on Muon ($g - 2$) lies in the TeV range, we consider $m_\eta \geq 600$ GeV for the DM analysis. In this region of parameter space, apart from annihilation and co-annihilation among the inert doublet components, we have additional co-annihilation channels of the inert doublet DM with ψ . The small mass difference required by the Muon ($g - 2$) excess makes the co-annihilation between DM and ψ significant. On the top right panel plot of Fig.(4) we plot the spin independent direct detection cross-sections with DM mass for the relic satisfied points. We show all the recent DM direct search limits from the XENON1T [40], PandaX-4t [41], XENONnT [42], LZ [43], and the proposed sensitivity limit from the upcoming experiments Darwin [44] and DarkSide-20K [45]. In the lower panel plot of Fig.(4) we show the allowed parameter spaces required to satisfy the correct DM relic and the observed Muon ($g - 2$) by the Fermi Lab. The cyan points generate the observed Muon $g - 2$ by the Fermi Lab while the red points satisfy the correct DM relic.

2.4 Leptogenesis

In this model, a net lepton asymmetry can not be generated from the decay of the lightest right handed neutrino (N_1) as there are no one loop diagram to generate the required CP

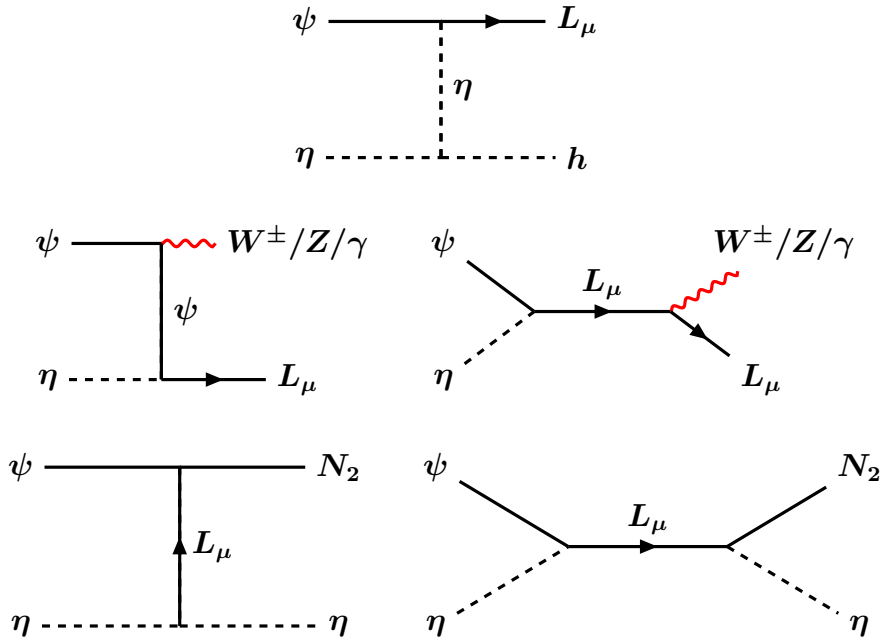


Figure 3: Co-annihilation channels of dark matter with triplet fermion ψ .

asymmetry. A net lepton asymmetry can be generated from the decay of the right handed neutrino N_2 and ψ . In case of hierarchical mass spectrum ($m_\psi \ll M_2$ or $M_2 \ll m_\psi$) the lepton asymmetry is mainly generated by the decay of the lightest fermion. The asymmetry produced from the decay of the heavier fermion is washed out by the inverse decay of the lighter one. If we take the hierarchy $m_\psi < M_2$ a lepton asymmetry is generated in muon/muonic neutrino from the decay of ψ . A few earlier works on leptogenesis from a triplet fermion can be found in [17, 46–48]. Being triplet, ψ has strong gauge scatterings that keep it in equilibrium up to a small temperature. It reduces the asymmetry production. This result in a high scale leptogenesis ($m_\psi \gtrsim 10^{10}$ GeV). Similarly if we take ($M_2 < m_\psi$) a lepton asymmetry can be generated in the muon/muonic neutrino from the decay of N_2 . In a scotogenic neutrino mass generation the Yukawa coupling of N_2 is always large enough resulting in a strong washout of asymmetry from the inverse decays. This region of parameter space is known as strong washout region ($\Gamma_{2,\psi}/H(T = M_2) \gtrsim 4$). In a strong washout region, it is impossible to have leptogenesis around the TeV scale with hierarchical mass spectrum [30]. To be consistent with Muon ($g - 2$) and Dark matter parameter space the only way to have TeV scale leptogenesis is to consider a resonant leptogenesis [10]. The resonant condition would be satisfied if $M_2 - m_\psi \simeq \Gamma_{2,\psi}/2$, $\Gamma_{2,\psi}$ being the decay width of N_2 and ψ respectively. In a resonant leptogenesis scenario since the masses of N_2 and ψ are similar, both can contribute to the production of a lepton asymmetry. The relevant tree level and self-energy diagram for generating CP asymmetry in N_2 and ψ decay are shown in Fig 5. The CP asymmetry parameters generated from the interference of tree level and one loop self-energy diagrams are given in Eq. 17.

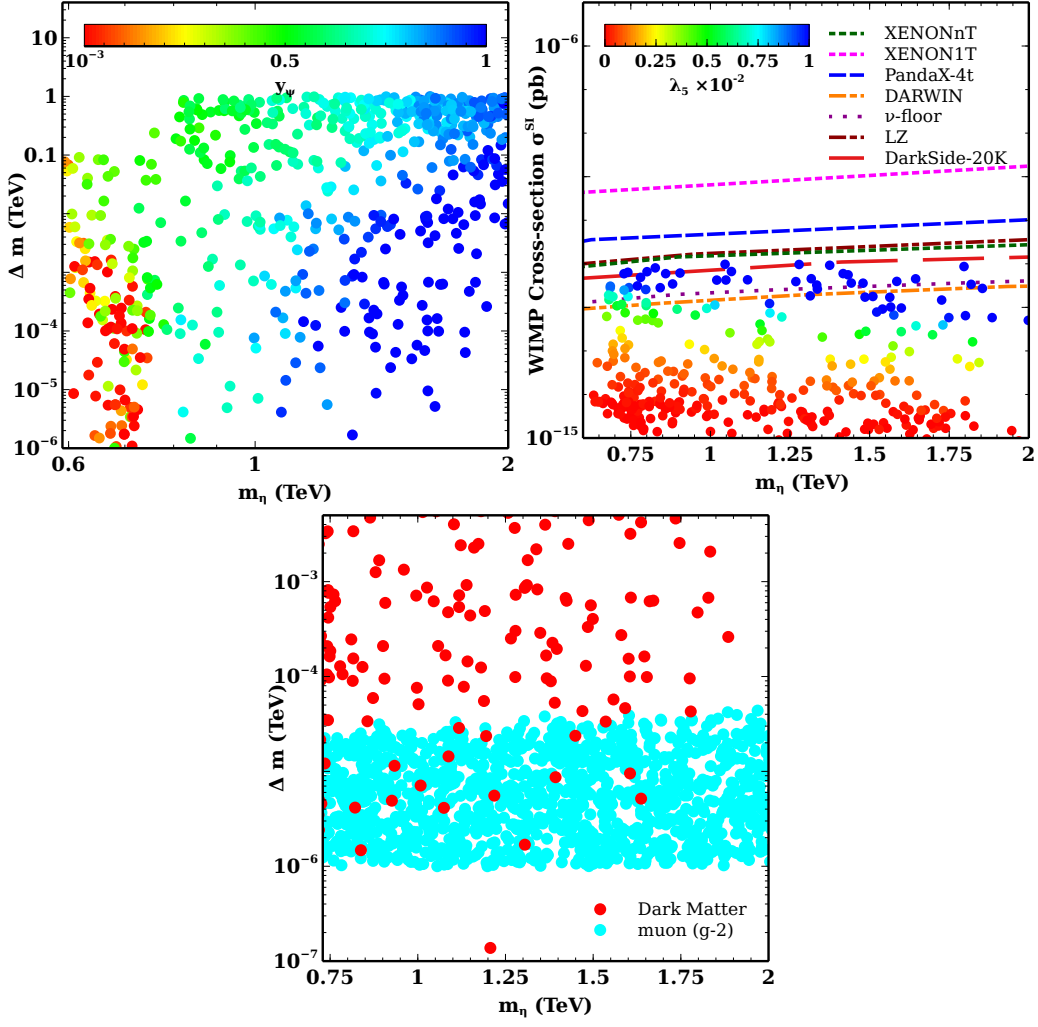


Figure 4: Scan plot showing the parameter space in $m_\eta - \Delta m$ plane with y_ψ as the color bar that satisfy the DM relic (upper left panel), DM spin independent direct detection cross-section (upper right panel) and common parameter space in $m_\eta - \Delta m$ plane for Muon ($g - 2$) and dark matter (lower panel). Here m_ψ is varied randomly from 0.6 TeV to 2 TeV and $m_\eta = m_\psi - \Delta m$, with Δm varied from 10^{-6} TeV to 1 TeV. The couplings λ_3, λ_4 and λ_5 are varied in the range $(10^{-5} - 1)$.

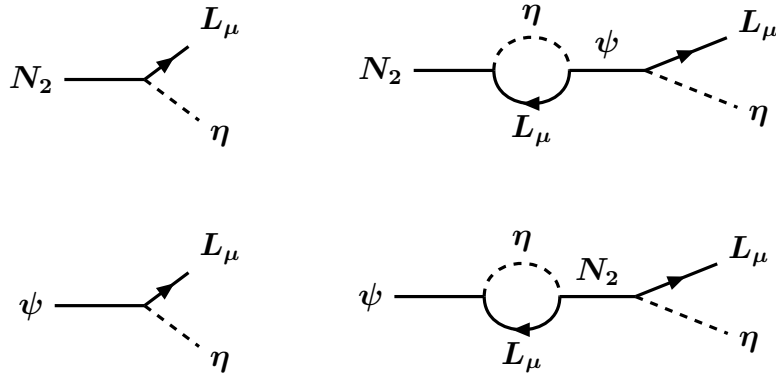


Figure 5: Tree level and one loop self-energy diagrams relevant for resonant leptogenesis.

$$\begin{aligned}
 \epsilon_{N_2} &= \frac{\text{Im}[(y_{\eta 2}^\dagger y_\psi)^2]}{(y_{\eta 2}^\dagger y_{\eta 2})(y_\psi^\dagger y_\psi)} \frac{(M_2^2 - m_\psi^2)M_2\Gamma_\psi}{(M_2^2 - m_\psi^2)^2 + M_2^2\Gamma_\psi^2}, \\
 \epsilon_\psi &= \frac{\text{Im}[(y_\psi^\dagger y_{\eta 2})^2]}{(y_{\eta 2}^\dagger y_{\eta 2})(y_\psi^\dagger y_\psi)} \frac{(m_\psi^2 - M_2^2)m_\psi\Gamma_{N_2}}{(m_\psi^2 - M_2^2)^2 + m_\psi^2\Gamma_{N_2}^2}.
 \end{aligned} \tag{17}$$

The relevant Boltzmann Equations for leptogenesis are

$$\begin{aligned}
\frac{dY_{N_2}}{dz} &= -D_{N_2}(Y_{N_2} - Y_{N_2}^{eq}), \\
\frac{dY_\psi}{dz} &= -D_\psi(Y_\psi - Y_\psi^{eq}) - S_A(Y_\psi^2 - (Y_\psi^{eq})^2), \\
\frac{dY_{B-L_\mu}}{dz} &= -\epsilon_{N_2}D_{N_2}(Y_{N_2} - Y_{N_2}^{eq}) - \epsilon_\psi D_\psi(Y_\psi - Y_\psi^{eq}) - W_{ID}^\psi Y_{B-L_\mu} \\
&\quad - W_{ID}^{N_2} Y_{B-L_\mu} - W_{\Delta L} Y_{B-L_\mu},
\end{aligned} \tag{18}$$

where the decay terms D_{N_2} and D_ψ are given by

$$D_{N_2} = K_{N_2}(z) \frac{\kappa_1(z)}{\kappa_2(z)}, \quad D_\psi = K_\psi(m_\psi/M_2 z) \frac{\kappa_1\left(\frac{m_\psi}{M_2} z\right)}{\kappa_2\left(\frac{m_\psi}{M_2} z\right)} \tag{19}$$

and K_{N_2} , K_ψ is written as

$$K_{N_2} = \frac{\Gamma_{N_2}}{H(T = M_2)}, \quad K_\psi = \frac{\Gamma_\psi}{H(T = m_\psi)}. \tag{20}$$

The decay widths Γ_{N_2} and Γ_ψ are given by

$$\Gamma_{N_2} = \frac{M_2}{8\pi} (y_{\eta_2}^\dagger y_{\eta_2}) \left(1 - \frac{m_\eta^2}{M_2^2}\right), \quad \Gamma_\psi = \frac{m_\psi}{8\pi} (y_\psi^\dagger y_\psi) \left(1 - \frac{m_\eta^2}{m_\psi^2}\right). \tag{21}$$

The terms $W_{ID}^{N_2}$ and W_{ID}^ψ are the washout terms due to the inverse decay of N_2 and ψ and are given by

$$W_{ID}^{N_2} = \frac{1}{4} K_{N_2}(z)^3 \kappa_1(z), \quad W_{ID}^\psi = \frac{1}{4} K_\psi(m_\psi/M_2 z)^3 \kappa_1\left(\frac{m_\psi}{M_2} z\right). \tag{22}$$

The term $W_{\Delta L}$ and takes care of the washouts coming from the lepton number violating scattering terms defined as $W_{\Delta L} = \Gamma/Hz^2$. The important scatterings in this model are $l_\mu \eta \rightarrow \bar{l}_\mu \eta^*$ and $l_\mu l_\mu \rightarrow \eta \eta^*$. The gauge boson mediated scattering term S_A for fermion triplet ψ is given by

$$S_A = \left(\frac{\pi^2 g^{*1/2} M_{Pl}}{1.66 * 180 g_\psi^2}\right) \frac{1}{m_\psi} \left(\frac{I_z}{m_\psi/M_2 z \kappa_2(m_\psi/M_2 z)^2}\right), \tag{23}$$

where the form of I_z is given as

$$I(z) = \int_4^\infty \sqrt{x} \kappa(m_\psi/M_2 z \sqrt{x}) \hat{\sigma}_A(x) dx. \tag{24}$$

Here, $\hat{\sigma}_A(x)$ is cross-section for gauge boson mediated processes given by [49]

$$\hat{\sigma}_A(x) = \frac{6g^2}{72\pi} \left[\frac{45}{2} r(x) - \frac{27}{2} r(x)^3 - \{9(r(x)^2 - 2) + 18(r(x)^2 - 1)^2\} \ln\left(\frac{1+r(x)}{1-r(x)}\right) \right], \tag{25}$$

with $r(x) = \sqrt{1 - 4/x}$.

2.4.1 Leptogenesis Results and Discussion

This section discusses the results of resonant leptogenesis from fermion triplet ψ and N_2 . By constraining the mass of triplet m_ψ and Yukawa coupling y_ψ from dark matter and Muon ($g - 2$) analysis, we solved the Boltzmann equations Eq. (18) for leptogenesis. In Fig. (6), we show the evolution of co-moving number density of N_2 , ψ and $B - L_\mu$ with $z = M_2/T$ for different benchmark values of λ_5 . The upper left panel plot shows that with an increase in λ_5 , the N_2 deviates more from its equilibrium. The quartic coupling λ_5 and the Yukawa couplings y_{η_2} contributes to the neutrino mass generation. With the increase in λ_5 the required value of the Yukawa couplings Y_{η_2} decreases. This lead to a decrease in the decay and inverse decay process resulting in a larger deviation from the equilibrium abundance. From the upper right panel plot, it can be seen that changes in the quartic coupling λ_5 does not affect the co-moving number density of ψ and it tracks its equilibrium abundance. It is because, ψ abundance is mainly determined by decay term D_ψ and scattering term S_A , both of which are independent of λ_5 . On the lower panel plot it can be seen that with the increase in λ_5 the $B - L_\mu$ asymmetry increases. Since, an increase in λ_5 , leads to a larger deviation from equilibrium abundance for N_2 , it results in an increase in the production of asymmetry.

In Fig. (7) we show the evolution of N_2 , ψ and $B - L_\mu$ asymmetry with $z = M_2/T$ with different benchmark values of y_ψ . In the upper left panel plot, we see that the N_2 nearly tracks its equilibrium abundance and the abundance does not change with the change in y_ψ . With the chosen $\lambda_5 = 10^{-3}$, the Yukawa couplings y_{η_2} are large enough to keep the N_2 close to its equilibrium abundance. As the y_ψ is not involved in the decay or inverse decay of N_2 , its abundance remains constant with the change in y_ψ . The top right panel shows that the ψ tracks its equilibrium irrespective of y_ψ . Although, a change in y_ψ changes the decay and inverse decay rate of ψ , its gauge annihilation always keeps it near equilibrium. In the lower panel plot of Fig. (7) it is observed that with the increase in y_ψ the $B - L_\mu$ asymmetry decreases. As y_ψ increases, the decay width of ψ as well as the CP asymmetry parameters ϵ_{N_2} and ϵ_ψ increase. However, it also results in strong washouts from the inverse decays and scatterings, decreasing $B - L_\mu$ asymmetry. The net lepton asymmetry generated in the muon sector is converted into baryon asymmetry via sphaleron factor $Y_B = c_{sph} Y_{B-L_\mu}$, where $c_{sph} = 33/57$ for our model. The details are given in Appendix (B).

In Fig. (8), we show a scan plot in m_ψ vs y_ψ plane (left) and m_η vs Δm plane (right) that satisfies Muon ($g - 2$), observed baryon asymmetry and DM relic. In the left panel plot, the cyan dot markers satisfy the observed Muon ($g - 2$), while the red star markers satisfy the observed baryon asymmetry as well as Muon ($g - 2$). The blue star markers satisfy the observed DM relic, direct detection bounds, observed BAU and observed excess of Muon ($g - 2$). In the right panel plot, the cyan dot markers satisfy the observed Muon ($g - 2$), while the red dot markers satisfy observed DM relic and direct detection bounds. The blue dot markers satisfy observed BAU also. The blue star points are also given in table (2).

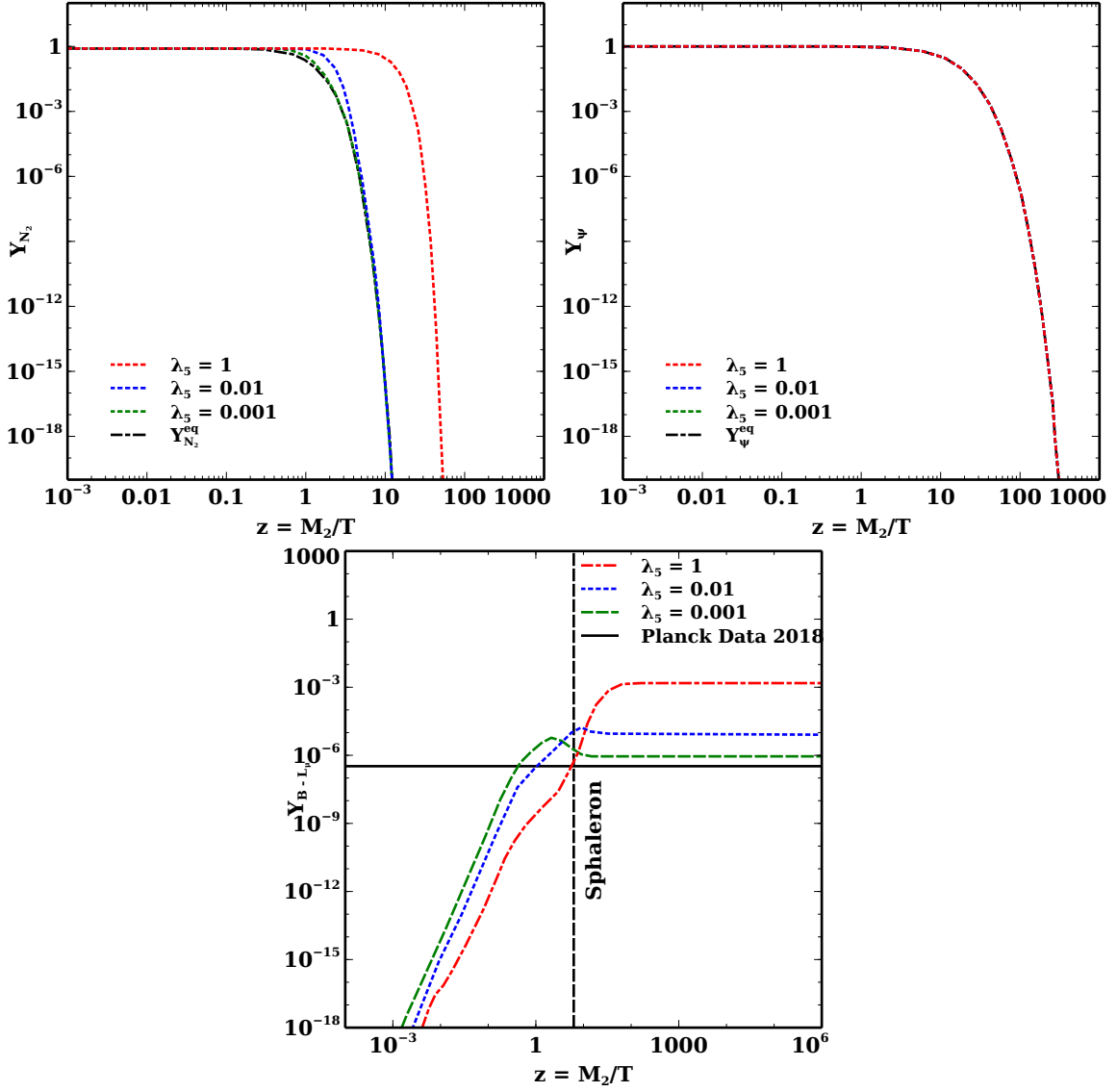


Figure 6: Variation of co moving number density Y_{N_2} (upper left panel), Y_ψ (upper right panel) and $B - L_\mu$ asymmetry (lower panel) with $z = M_2/T$ for different benchmark values of the quartic coupling λ_5 . The other parameters are fixed at $M_1 = 7.9 \times 10^{-1}$ TeV, $M_2 = 8 \times 10^{-1}$ TeV, $M_3 = 9 \times 10^{-1}$ TeV, $m_\eta = 7.9 \times 10^{-1}$ TeV, $m_1 = 10^{-13}$ eV, $m_\psi = 8 \times 10^{-1}$ TeV and $y_\psi = 2 \times 10^{-3}$. The horizontal lines in right panel plot depicts the required $B - L_\mu$ asymmetry to generate net baryon asymmetry of the Universe (Planck Data 2018) after sphaleron transition (Vertical dotted line).

m_ψ (TeV)	m_η (TeV)	y_ψ	M_2 (TeV)	λ_5	ϵ_ψ	ϵ_{N_2}
0.75	0.749997	0.02	0.7500000005	0.009	3.5×10^{-7}	0.094
0.76	0.759999	0.001	0.7600001	0.03	1.9×10^{-10}	3.9×10^{-7}
0.77	0.769999	0.01	0.7700001	0.02	2.9×10^{-10}	3.9×10^{-5}
0.78	0.779998	0.03	0.7800000009	0.003	4×10^{-7}	0.078
0.8	0.799998	0.009	0.800000001	0.002	5.63×10^{-7}	0.0064
0.81	0.809995	0.02	0.8100000006	0.03	1.58×10^{-7}	0.129

Table 2: Benchmark points that satisfy leptogenesis, dark matter and Muon ($g - 2$) anomaly simultaneously.

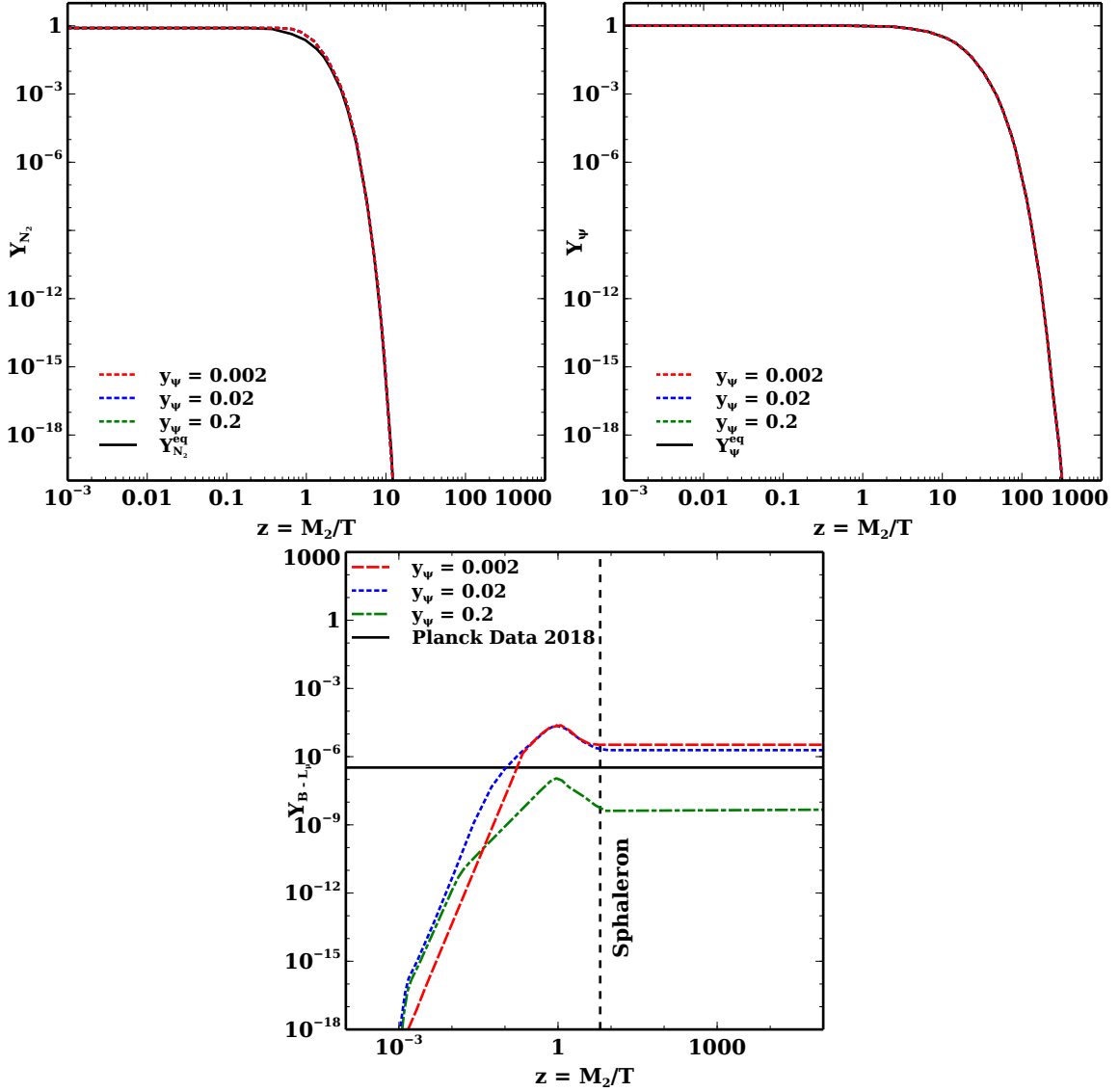


Figure 7: Variation of co moving number density Y_{N_2} (upper left panel), Y_ψ (upper right panel) and $B - L_\mu$ asymmetry (lower panel) with $z = M_2/T$ for different benchmark values of the Yukawa couplings y_ψ . The other parameters are fixed at $M_1 = 7.9 \times 10^{-1}$ TeV, $M_2 = 0.8$ TeV, $\Delta m_{N_2\psi} = 10^{-10}$ TeV, $M_3 = 0.9$ TeV, $m_\eta = 7.9 \times 10^{-1}$ TeV, $m_1 = 10^{-13}$ eV, $m_\psi = 0.8$ TeV and $\lambda_5 = 10^{-3}$. The horizontal lines in right panel plot depicts the required $B - L_\mu$ asymmetry to generate net baryon asymmetry of the Universe (Planck Data 2018) after the sphaleron transition (Vertical dotted line).

3 Conclusions

We propose a minimal extension of the scotogenic model that has the potential to explain non-zero neutrino mass, Muon ($g - 2$) along with dark matter and baryon asymmetry of the Universe. Three copies of Majorana right-handed neutrinos generate the light neutrino masses through the scotogenic mechanism. Because of the imposed Z_4 symmetry, the Z_2 odd fermion triplet can provide a one-loop contribution to the muon's anomalous magnetic moment. The fermion triplet can also generate net lepton asymmetry in the muon sector through its out-of-equilibrium decay. The Yukawa coupling involved in leptogenesis is free from neutrino sector. The strong gauge annihilation keeps the triplet fermion abundance close to its equilibrium abundance. The Yukawa couplings of N_2 are large enough and un-

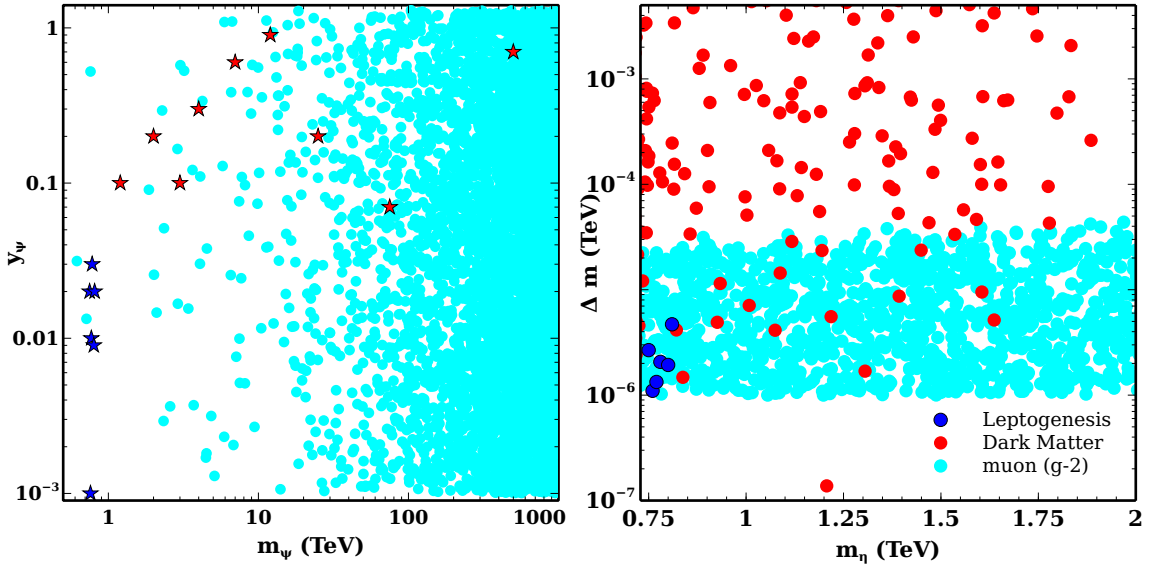


Figure 8: Scan plot in $m_\psi - y_\psi$ plane (left). Here cyan points satisfy Muon ($g - 2$) and the red stars represent points that satisfy Muon ($g - 2$) and observed BAU. The blue star points satisfy DM relic, direct detection limit, BAU and FNL results on Muon ($g - 2$). Parameter space in $m_\eta - \Delta m$ plane (right). Here cyan points satisfy Muon ($g - 2$), red points satisfy dark matter and direct detection limit and blue data points satisfy BAU also.

dergo strong washouts by the inverse decays. Both these factors reduce the lepton asymmetry production. It leads to a high-scale leptogenesis around $\sim 10^{10}$ GeV. To successfully generate the lepton asymmetry around the TeV scale, we consider the resonance enhancement of asymmetry between ψ and N_2 . The Yukawa coupling involved in leptogenesis y_ψ , also contributes to the Muon ($g - 2$) and provides a strong correlation between the two. The co-annihilation of the DM, η with the triplet fermion ψ is significant in getting the correct DM relic. The mass difference between the triplet fermion and the doublet scalar becomes a crucial parameter. Both Muon ($g - 2$) and DM relic favors towards a parameter space where $m_\psi \sim m_{DM}$. The requirement of correct asymmetry at the TeV scale necessarily imposes the resonance condition $M_2 - m_\psi \sim \Gamma_{2,\psi}/2$.

As the scale of triplet fermion involved in leptogenesis is in the TeV range, the model is testable in future LHC experiments. The ATLAS experiment at LHC has obtained a lower limit on the mass of heavy fermion triplets around 750 GeV at 95% confidence level [50]. The phenomenology of inert scalar doublet as dark matter is also discussed in the paper. We constrained our model by the recent relic density results and direct detection bounds. We show that rich phenomenology among the Muon ($g - 2$) observed excess, leptogenesis and DM production around the TeV scale. Such low-scale models may be tested near future experiments.

Acknowledgments

B. C. Chauhan is thankful to the Inter-University Centre for Astronomy and Astrophysics (IUCAA) for providing the necessary facilities during the completion of this work.

A Cross-sections for the dark matter co-annihilation

Here we show the cross-sections of the dark matter co-annihilation,

$$\begin{aligned}
\sigma_{\eta\psi \rightarrow L\mu h} = & -\frac{1}{16\pi \left(-4m_\psi^2 m_\eta^2 + (-m_\psi^2 - m_\eta^2 + s)^2 \right)} \left[\right. \\
& \left(-((\lambda_3 + \lambda_4 + \lambda_5)v)^2 \left(\frac{-y_\psi}{2} \right) \left(\frac{-y_\psi}{2} \right) \right) \\
& - \left(4(m_\psi^2 - m_\eta^2 + 2m_\psi m_\mu + m_\mu^2) s^3 \right) \\
& \times \frac{1}{\sqrt{\frac{1}{s^4} (m_\psi^4 + (m_\eta^2 - s)^2 - 2m_\psi^2 (m_\eta^2 + s)) (m_h^4 + (m_\mu^2 - s)^2 - 2m_h^2 (m_\mu^2 + s))}} \\
& \times \frac{1}{(m_\eta^2 m_\mu^2 - m_\eta^2 s + m_\mu^2 s - s^2 + m_h^2 (-m_\eta^2 + s) + m_\psi^2 (m_h^2 - m_\mu^2 + s))} \\
& \times \frac{1}{(s^2 \sqrt{\frac{1}{s^4} (m_\psi^4 + (m_\eta^2 - s)^2 - 2m_\psi^2 (m_\eta^2 + s)) (m_h^4 + (m_\mu^2 - s)^2 - 2m_h^2 (m_\mu^2 + s))}} \\
& + \log \left(\frac{m_\eta^2 m_\mu^2 - m_\eta^2 s + m_\mu^2 s - s^2 + m_h^2 (-m_\eta^2 + s) + m_\psi^2 (m_h^2 - m_\mu^2 + s)}{s^2 \sqrt{\frac{1}{s^4} (m_\psi^4 + (m_\eta^2 - s)^2 - 2m_\psi^2 (m_\eta^2 + s)) (m_h^4 + (m_\mu^2 - s)^2 - 2m_h^2 (m_\mu^2 + s))}} \right) \\
& \left. - \log \left(\frac{m_\eta^2 m_\mu^2 - m_\eta^2 s + m_\mu^2 s - s^2 + m_h^2 (-m_\eta^2 + s) + m_\psi^2 (m_h^2 - m_\mu^2 + s) - s^2}{\sqrt{\frac{1}{s^4} (m_\psi^4 + (m_\eta^2 - s)^2 - 2m_\psi^2 (m_\eta^2 + s)) (m_h^4 + (m_\mu^2 - s)^2 - 2m_h^2 (m_\mu^2 + s))}} \right) \right], \\
\sigma_{\psi\eta \rightarrow N_2\eta} = & \frac{1}{16\pi (-4m_\psi^2 m_\eta^2 + (-m_\psi^2 - m_\eta^2 + s)^2)} \left[\frac{1}{(m_\mu^2 - s)^2} \right. \\
& \times \sqrt{\frac{1}{s^4} ((m_\psi^4 + (m_\eta^2 - s)^2 - 2m_\psi^2 (m_\eta^2 + s)) (m_\eta^4 + (M_2^2 - s)^2 - 2m_\eta^2 (M_2^2 + s)))} \\
& \times \left(4m_\psi s (-m_\eta^2 m_\mu + (M_2 + m_\mu)(M_2 m_\mu + s)) + (m_\eta^2 - s)(-4M_2 m_\mu s + m_\eta^2 (m_\mu^2 + s) \right. \\
& \left. - M_2^2 (m_\mu^2 + s) - s(m_\mu^2 + s)) + m_\psi^2 (4M_2 m_\mu s - m_\eta^2 (m_\mu^2 + s) + M_2^2 (m_\mu^2 + s) \right. \\
& \left. + s(m_\mu^2 + s)) \right) \times \left(\frac{-y_\psi}{\sqrt{2}} \right)^2 \left(\frac{-y_{\eta_2}}{\sqrt{2}} \right)^2 + \frac{1}{(m_\mu^2 - s)^2} \\
& \times \sqrt{\frac{1}{s^4} ((m_\psi^4 + (m_\eta^2 - s)^2 - 2m_\psi^2 (m_\eta^2 + s)) (m_\eta^4 + (M_2^2 - s)^2 - 2m_\eta^2 (M_2^2 + s)))} \\
& \times \left(4m_\psi s (-m_\eta^2 m_\mu + (M_2 + m_\mu)(M_2 m_\mu + s)) + (m_\eta^2 - s)(-4M_2 m_\mu s + m_\eta^2 (m_\mu^2 + s) \right. \\
& \left. - M_2^2 (m_\mu^2 + s) - s(m_\mu^2 + s)) + m_\psi^2 (4M_2 m_\mu s - m_\eta^2 (m_\mu^2 + s) + M_2^2 (m_\mu^2 + s) + s(m_\mu^2 + s)) \right) \\
& \times \left(\frac{-y_\psi}{\sqrt{2}} \frac{-y_{\eta_2}}{\sqrt{2}} \frac{-y_\psi}{\sqrt{2}} \frac{-y_{\eta_2}}{\sqrt{2}} \right) + 2 \left(\frac{-y_\psi}{\sqrt{2}} \frac{-y_{\eta_2}}{\sqrt{2}} \frac{-y_\psi}{\sqrt{2}} \frac{-y_{\eta_2}}{\sqrt{2}} \right) \\
& \times \left(- \left(4(m_\psi^2 - m_\eta^2 + 2m_\psi m_\mu + m_\mu^2) (m_\eta^2 - (M_2 + m_\mu)^2) s^3 \right) \right. \\
& \times \sqrt{\frac{1}{s^4} (m_\psi^4 + (m_\eta^2 - s)^2 - 2m_\psi^2 (m_\eta^2 + s)) (m_\eta^4 + (M_2^2 - s)^2 - 2m_\eta^2 (M_2^2 + s)) /} \\
& \left(-m_\eta^4 + m_\eta^2 (M_2^2 - 2s) + m_\psi^2 (m_\eta^2 - M_2^2 - s) + s(-M_2^2 + 2m_\mu^2 + s) \right. \\
& \left. - s \sqrt{\frac{1}{s^4} (m_\psi^4 + (m_\eta^2 - s)^2 - 2m_\psi^2 (m_\eta^2 + s)) (m_\eta^4 + (M_2^2 - s)^2 - 2m_\eta^2 (M_2^2 + s))} \right) \left. \right)
\end{aligned}$$

$$\begin{aligned}
\sigma_{\eta\psi \rightarrow L\mu Z} = & \frac{1}{16\pi(-4m_\psi^2 m_{\eta R}^2 + (-m_\psi^2 - m_{\eta R}^2 + s)^2)} \left[EE^2(-1/(m_\mu^2 - s)^2 2(m_Z^2 - m_\nu^2 - s) \right. \\
& \times \sqrt{\frac{1}{s^4}(m_\psi^4 + (m_{\eta R}^2 - s)^2 - 2m_\psi^2(m_{\eta R}^2 + s))(m_Z^4 + (m_\nu^2 - s)^2 - 2m_Z^2(m_\nu^2 + s))} \\
& \times (4m_\psi m_\mu s + m_\psi^2(m_\mu^2 + s) - (m_{\eta R}^2 - s)(m_\mu^2 + s)) \\
& \times \left(-0.25 \frac{\cos_w}{\sin_w} + \frac{\sin_w}{\cos_w} \right)^2 \left(\frac{-y_\psi - y_\psi}{\sqrt{2}} \frac{y_\psi}{\sqrt{2}} \right) - \left(\frac{-y_\psi}{\sqrt{2}} \frac{y_\psi}{\sqrt{2}} \right) \left(\frac{\cos_w^2 + \sin_w^2}{2\cos_w \sin_w} \right)^2 \\
& \times ((2s\sqrt{\frac{1}{s^4}(m_\psi^4 + (m_{\eta R}^2 - s)^2 - 2m_\psi^2(m_{\eta R}^2 + s))(m_Z^4 + (m_\mu^2 - s)^2 - 2m_Z^2(m_\mu^2 + s))} \\
& \times (4m_\psi(-2m_{\eta I}^2 - 2m_{\eta R}^2 + m_Z^2)m_\mu s^2 + m_\psi^4(m_Z^2 - m_\mu^2 + s)^2 \\
& + m_{\eta R}^4(-m_Z^2 + m_\mu^2 + s)^2 - 2m_{\eta R}^2 s(m_Z^4 - m_\mu^4 - 2m_{\eta I}^2(m_Z^2 - m_\mu^2) - 2m_Z^2 s + 2m_\mu^2 s + s^2) \\
& + s^2(8m_{\eta I}^4 + m_Z^4 + m_\mu^4 + m_Z^2(4m_\mu^2 - 2s) - 2m_\mu^2 s + s^2 + m_{\eta I}^2(-6m_Z^2 - 8m_\mu^2 + 4s) \\
& - 1/s^2(m_\psi^4 + (m_{\eta R}^2 - s)^2 - 2m_\psi^2(m_{\eta R}^2 + s))(m_Z^4 + (m_\mu^2 - s)^2 \\
& - 2m_Z^2(m_\mu^2 + s))) - 2m_\psi^2(m_{\eta R}^2(m_Z^4 - 2m_Z^2 m_\mu^2 + m_\mu^4 + s^2) + \\
& + s(-m_Z^4 + (m_\mu^2 - s)^2 - m_Z^2 s + 2m_{\eta I}^2(m_Z^2 - m_\mu^2 + 2s)))))/ \\
& ((m_\psi^2(m_Z^2 - m_\mu^2 + s) + m_{\eta R}^2(-m_Z^2 + m_\mu^2 + s) + \\
& s(-2m_{\eta I}^2 + m_Z^2 + m_\mu^2 - s \\
& - s\sqrt{\frac{1}{s^4}(m_\psi^4 + (m_{\eta R}^2 - s)^2 - 2m_\psi^2(m_{\eta R}^2 + s))(m_Z^4 + (m_\mu^2 - s)^2 - 2m_Z^2(m_\mu^2 + s))}) \\
& \times (m_\psi^2(m_Z^2 - m_\mu^2 + s) + m_{\eta R}^2(-m_Z^2 + m_\mu^2 + s) + s(-2m_{\eta I}^2 + m_Z^2 + m_\mu^2 - s \\
& + s\sqrt{\frac{1}{s^4}(m_\psi^4 + (m_{\eta R}^2 - s)^2 - 2m_\psi^2(m_{\eta R}^2 + s))(m_Z^4 + (m_\mu^2 - s)^2 - 2m_Z^2(m_\mu^2 + s))})) \\
& + (2m_\psi^2 - 4m_{\eta I}^2 - 2m_{\eta R}^2 + m_Z^2 + 4m_\psi m_\mu + 2m_\mu^2) \\
& \times \log \left[(m_\psi^2(m_Z^2 - m_\mu^2 + s) + m_{\eta R}^2(-m_Z^2 + m_\mu^2 + s) + s(-2m_{\eta I}^2 + m_Z^2 + m_\mu^2 - s \right. \\
& - s\sqrt{\frac{1}{s^4}(m_\psi^4 + (m_{\eta R}^2 - s)^2 - 2m_\psi^2(m_{\eta R}^2 + s))(m_Z^4 + (m_\mu^2 - s)^2 - 2m_Z^2(m_\mu^2 + s))})/ \\
& (m_\psi^2(m_Z^2 - m_\mu^2 + s) + m_{\eta R}^2(-m_Z^2 + m_\mu^2 + s) + s(-2m_{\eta I}^2 + m_Z^2 + m_\mu^2 - s \\
& + s\sqrt{\frac{1}{s^4}(m_\psi^4 + (m_{\eta R}^2 - s)^2 - 2m_\psi^2(m_{\eta R}^2 + s))(m_Z^4 + (m_\mu^2 - s)^2 - 2m_Z^2(m_\mu^2 + s))})) \left. \right] \\
& + 1/(m_\mu^2 - s)^2 - 0.25 \times \left(\frac{\cos_w}{\sin_w} + \frac{\sin_w}{\cos_w} \right) \left(\frac{-y_\psi}{\sqrt{2}} \right) \left(\frac{-y_\psi}{\sqrt{2}} \right) \left(\frac{\cos_w^2 + \sin_w^2}{2\cos_w \sin_w} \right) \\
& \times ((-2m_\psi^2 + 2m_{\eta R}^2 - 2m_\psi m_\mu + m_\mu^2 - s) \\
& \times s\sqrt{\frac{1}{s^4}(m_\psi^4 + (m_{\eta R}^2 - s)^2 - 2m_\psi^2(m_{\eta R}^2 + s))(m_Z^4 + (m_\mu^2 - s)^2 - 2m_Z^2(m_\mu^2 + s))} \\
& + (-2m_\psi^4 - 4m_\psi^3 m_\mu + m_{\eta I}^2(-2m_{\eta R}^2 - m_\mu^2 + s) + m_\psi^2(2m_{\eta I}^2 + 2m_{\eta R}^2 - 2m_Z^2 - m_\mu^2 + s) \\
& + m_\mu^2(m_\mu^2 + s) + 2m_\psi m_\mu(m_{\eta I}^2 + m_{\eta R}^2 - m_Z^2 + m_\mu^2 + s)) \\
& \log \left[(m_\psi^2(m_Z^2 - m_\mu^2 + s) + m_{\eta R}^2(-m_Z^2 + m_\mu^2 + s) + s(-2m_{\eta I}^2 + m_Z^2 + m_\mu^2 - s \right. \\
& - s\sqrt{\frac{1}{s^4}(m_\psi^4 + (m_{\eta R}^2 - s)^2 - 2m_\psi^2(m_{\eta R}^2 + s))(m_Z^4 + (m_\mu^2 - s)^2 - 2m_Z^2(m_\mu^2 + s))})/
\end{aligned}$$

(27)

$$\begin{aligned}
& (m_\psi^2(m_Z^2 - m_\mu^2 + s) + m_{\eta_R}^2(-m_Z^2 + m_\mu^2 + s) + s(-2m_{\eta_I}^2 + m_Z^2 + m_\mu^2 - s \\
& + s\sqrt{\frac{1}{s^4}(m_\psi^4 + (m_{\eta_R}^2 - s)^2 - 2m_\psi^2(m_{\eta_R}^2 + s))(m_Z^4 + (m_\mu^2 - s)^2 - 2m_Z^2(m_\mu^2 + s))}) \\
& + 2\left(-2 \times \frac{\sin w}{\cos w}\right)^2 \left(\frac{-y_\psi}{\sqrt{2}}\right) \left(\frac{-y_\psi}{\sqrt{2}}\right) ((4(6m_\psi^2 - m_Z^2)(m_\psi^2 - m_{\eta_R}^2 + 2m_\psi m_\mu + m_\mu^2)s^3 \\
& \times \sqrt{\frac{1}{s^4}(m_\psi^4 + (m_{\eta_R}^2 - s)^2 - 2m_\psi^2(m_{\eta_R}^2 + s))(m_Z^4 + (m_\mu^2 - s)^2 - 2m_Z^2(m_\mu^2 + s))}) / \\
& ((m_\psi^2(m_Z^2 - m_\mu^2 + s) - m_{\eta_R}^2(m_Z^2 - m_\mu^2 + s) + s(-m_Z^2 - m_\mu^2 + s \\
& + s\sqrt{\frac{1}{s^4}(m_\psi^4 + (m_{\eta_R}^2 - s)^2 - 2m_\psi^2(m_{\eta_R}^2 + s))(m_Z^4 + (m_\mu^2 - s)^2 - 2m_Z^2(m_\mu^2 + s))}) \\
& \times (m_\psi^2(m_Z^2 - m_\mu^2 + s) - m_{\eta_R}^2(m_Z^2 - m_\mu^2 + s) - s(m_Z^2 + m_\mu^2 \\
& + s(-1 + \sqrt{\frac{1}{s^4}(m_\psi^4 + (m_{\eta_R}^2 - s)^2 - 2m_\psi^2(m_{\eta_R}^2 + s))(m_Z^4 + (m_\mu^2 - s)^2 - 2m_Z^2(m_\mu^2 + s))})) \\
& - (6m_\psi^2 + 6m_\psi m_\mu + m_\mu^2 - s) \\
& \times \log\left[(-m_\psi^2(m_Z^2 - m_\mu^2 + s) + m_{\eta_R}^2(m_Z^2 - m_\mu^2 + s) + s(m_Z^2 + m_\mu^2 \right. \\
& (-m_\psi^2(m_Z^2 - m_\mu^2 + s) + m_{\eta_R}^2(m_Z^2 - m_\mu^2 + s) + s(m_Z^2 + m_\mu^2 \\
& + s(-1 + \sqrt{(1/(s^4))(m_\psi^4 + (m_{\eta_R}^2 - s)^2 - 2m_\psi^2(m_{\eta_R}^2 + s))(m_Z^4 + (m_\mu^2 - s)^2 - 2m_Z^2(m_\mu^2 + s))})) \\
& - \left(\frac{1}{m_\mu^2 - s}\right) 4\left(-2\frac{\sin w}{\cos w}\right) \left(-0.25\frac{\cos w}{\sin w} + \frac{\sin w}{\cos w}\right) \left(\frac{-y_\psi}{\sqrt{2}}\right) \left(\frac{-y_\psi}{\sqrt{2}}\right) \\
& \times (s(m_\psi^2 - m_{\eta_R}^2 + 3m_\psi m_\mu + m_\mu^2 + s) \\
& \sqrt{(1/(s^4))(m_\psi^4 + (m_{\eta_R}^2 - s)^2 - 2m_\psi^2(m_{\eta_R}^2 + s))(m_Z^4 + (m_\mu^2 - s)^2 - 2m_Z^2(m_\mu^2 + s))} \\
& - (m_\psi^4 + m_{\eta_R}^4 + 6m_\psi^3 m_\mu + m_\mu^2(-m_Z^2 + s) - m_{\eta_R}^2(m_\mu^2 + s) \\
& + m_\psi m_\mu(-6m_{\eta_R}^2 - 2m_Z^2 + 3(m_\mu^2 + s)) - m_\psi^2(2m_{\eta_R}^2 + m_Z^2 \\
& - 2(4m_\mu^2 + s))) \log\left[(-m_\psi^2(m_Z^2 - m_\mu^2 + s) + m_{\eta_R}^2(m_Z^2 - m_\mu^2 + s) + s(m_Z^2 \\
& + m_\mu^2 - s(1 + \sqrt{\frac{1}{s^4}(m_\psi^4 + (m_{\eta_R}^2 - s)^2 - 2m_\psi^2(m_{\eta_R}^2 + s))(m_Z^4 + (m_\mu^2 - s)^2 - 2m_Z^2(m_\mu^2 + s))})) / \\
& (-m_\psi^2(m_Z^2 - m_\mu^2 + s) + m_{\eta_R}^2(m_Z^2 - m_\mu^2 + s) + s(m_Z^2 + m_\mu^2 + s \\
& \times (-1 + \sqrt{\frac{1}{s^4}(m_\psi^4 + (m_{\eta_R}^2 - s)^2 - 2m_\psi^2(m_{\eta_R}^2 + s))(m_Z^4 + (m_\mu^2 - s)^2 - 2m_Z^2(m_\mu^2 + s))})) \right] \Big] \Big] \\
& \left. \right) - s(1
\end{aligned}$$

The general form for the thermally averaged annihilation cross-section is

$$\langle \sigma v \rangle_{AB} = \frac{1}{2T m_A^2 m_B^2 \kappa_2(m_A/T) \kappa_2(m_B/T)} \int_{(m_A+m_B)^2}^{\infty} \sigma_{AB \rightarrow CD} \quad (28)$$

$$(s - (m_A + m_B)^2) \sqrt{s} \kappa_1(\sqrt{s}/T). \quad (29)$$

Here $\sigma_{AB \rightarrow CD}$ is the cross section for the process $A + B \rightarrow C + D$, $\kappa_i s$ are modified Bessel functions of order i and T is the temperature.

B Calculation of sphaleron conversion factor

Here we derive the calculation of sphaleron conversion factor in our model according to the standard procedure described in [51]. For a relativistic particle X with spin s and degrees of freedom (dof) g_X , the relationship between the particle-antiparticle asymmetry and the particle's chemical potential is expressed as

$$Y_X - Y_{\bar{X}} = \frac{g_X T^2}{6} \begin{cases} \mu_X & \text{for fermions} \\ 2\mu_X & \text{for bosons} \end{cases} \quad (30)$$

The number of chemical potentials (or asymmetries) corresponds to the number of distinct particle species present in the plasma. However, this number is significantly reduced by constraints arising from chemical equilibrium conditions and conservation laws that govern the early universe as:

1. All the gauge bosons have vanishing chemical potential, imposing the equality of chemical potentials among electroweak and color multiplets.
2. Regardless of the temperature of the universe, the electric charge must be conserved, leading to the following constraint,

$$Q = \sum_i^{N_f} (\mu_{Q_i} + 2\mu_{u_i} - \mu_{d_i} - \mu_{l_i} - \mu_{e_i}) + \sum_i^m 2\mu_\phi + \sum_i^n 6\mu_{\psi_i} = 0. \quad (31)$$

Here, $\mu_{Q_i}, \mu_{u_i}, \mu_{d_i}, \mu_{l_i}$ and μ_{e_i} represent the chemical potentials for left-handed quark doublets, right-handed up-type quarks, right-handed down-type quarks, left-handed lepton doublets, right-handed charged leptons, respectively. The parameter N_f denotes the number of fermion generations present in the model. Similarly, μ_ϕ and μ_{ψ_i} represent the chemical potential for the scalar doublets and the fermion triplet, respectively, where m and n indicate the number of scalar doublets and the number of fermion triplet generations in the model.

3. Non-perturbative electroweak sphaleron and QCD instanton processes, while in thermal equilibrium, imposes the following constraints

$$\sum_i^{N_f} (3\mu_{Q_i} + \mu_{l_i}) = 0, \quad (32)$$

$$\sum_i^{N_f} (2\mu_{Q_i} - \mu_{d_i} - \mu_{u_i}) = 0 \quad (33)$$

4. All the SM Yukawa interactions and electroweak sphalerons in equilibrium also impose certain conditions as:

$$\begin{aligned} \mu_{u_i} - \mu_{Q_i} - \mu_\phi &= 0, & \phi^0 &\longleftrightarrow \bar{u}_L + u_R, \\ \mu_{d_i} - \mu_{Q_i} + \mu_\phi &= 0, & \phi^0 &\longleftrightarrow \bar{d}_R + d_L, \\ \mu_{e_i} - \mu_{l_i} + \mu_\phi &= 0, & \phi^0 &\longleftrightarrow \bar{e}_{iR} + e_{iL}, \\ \mu_{\psi_i} - \mu_{l_i} - \mu_\phi &= 0, & \psi^0 &\longleftrightarrow \phi^0 + l_{iL}. \end{aligned} \quad (34)$$

Assuming equilibrium among different generations, the generation index i can be dropped from the above equations. Replacing $\mu_{u_i}, \mu_{d_i}, \mu_{e_i}$ and μ_{ψ_i} in Eq. (31), μ_ϕ can be expressed in terms of $\mu_{Q_i} \equiv \mu_Q$ as

$$\mu_\phi = -\frac{8N_f - 18n}{4N_f + 2m + 6n}\mu_Q. \quad (35)$$

The Baryon number B in terms of chemical potential is written as

$$B = \sum_i^{N_f} (2\mu_{Q_i} + \mu_{u_i} + \mu_{d_i}) = 4N_f\mu_Q. \quad (36)$$

Similarly, the lepton number for muon is written as:

$$L_\mu = (2\mu_{l_\mu} + \mu_{\mu_R}) = -9\mu_Q + \left[\frac{(8N_f - 18n)}{(4N_f + 2m + 6n)} \right] \mu_Q. \quad (37)$$

From Eq. (36) and Eq. (37), we can write

$$\begin{aligned} B &= -\frac{16N_f^2 + 8mN_f + 24nN_f}{28N_f + 18m + 72n}L_\mu, \\ B &= \frac{16N_f^2 + 8mN_f + 24nN_f}{16N_f^2 + 18mN_f + 24nN_f + 28N_f + 18m + 72n}B - L_\mu. \end{aligned} \quad (38)$$

For our model, with $N_f = 3$, $m = 2$ and $n = 1$, $B = \frac{33}{57}(B - L_\mu)$.

References

- [1] N. Aghanim et al. Planck 2018 results. VI. Cosmological parameters. Astron. Astrophys., 641:A6, 2020. [Erratum: Astron. Astrophys. 652, C4 (2021)].
- [2] A. D. Sakharov. Violation of CP Invariance, C asymmetry, and baryon asymmetry of the universe. Pisma Zh. Eksp. Teor. Fiz., 5:32–35, 1967.
- [3] W. Buchmuller, P. Di Bari, and M. Plumacher. Leptogenesis for pedestrians. Annals Phys., 315:305–351, 2005.
- [4] Sacha Davidson, Enrico Nardi, and Yosef Nir. Leptogenesis. Phys. Rept., 466:105–177, 2008.
- [5] Apostolos Pilaftsis. The Little Review on Leptogenesis. J. Phys. Conf. Ser., 171:012017, 2009.
- [6] S. Yu. Khlebnikov and M. E. Shaposhnikov. The Statistical Theory of Anomalous Fermion Number Nonconservation. Nucl. Phys. B, 308:885–912, 1988.
- [7] Peter Minkowski. $\mu \rightarrow e\gamma$ at a Rate of One Out of 10^9 Muon Decays? Phys. Lett. B, 67:421–428, 1977.
- [8] Rabindra N. Mohapatra and Goran Senjanovic. Neutrino Masses and Mixings in Gauge Models with Spontaneous Parity Violation. Phys. Rev. D, 23:165, 1981.

- [9] Thomas Hugle, Moritz Platscher, and Kai Schmitz. Low-Scale Leptogenesis in the Scotogenic Neutrino Mass Model. Phys. Rev. D, 98(2):023020, 2018.
- [10] Apostolos Pilaftsis and Thomas E. J. Underwood. Resonant leptogenesis. Nucl. Phys. B, 692:303–345, 2004.
- [11] Apostolos Pilaftsis and Thomas E. J. Underwood. Electroweak-scale resonant leptogenesis. Phys. Rev. D, 72:113001, 2005.
- [12] Thomas Hambye. Leptogenesis at the TeV scale. Nucl. Phys. B, 633:171–192, 2002.
- [13] P. S. Bhupal Dev. TeV Scale Leptogenesis. Springer Proc. Phys., 174:245–253, 2016.
- [14] Debasish Borah, Arnab Dasgupta, and Devabrat Mahanta. TeV scale resonant leptogenesis with $L\mu$ - $L\tau$ gauge symmetry in light of the muon g -2. Phys. Rev. D, 104(7):075006, 2021.
- [15] Debasish Borah, Arnab Dasgupta, and Devabrat Mahanta. Dark sector assisted low scale leptogenesis from three body decay. Phys. Rev. D, 105(1):015015, 2022.
- [16] Devabrat Mahanta and Debasish Borah. Low scale Dirac leptogenesis and dark matter with observable ΔN_{eff} . Eur. Phys. J. C, 82(5):495, 2022.
- [17] Labh Singh, Devabrat Mahanta, and Surender Verma. Low scale leptogenesis in singlet-triplet scotogenic model. JCAP, 02:041, 2024.
- [18] Pasquale Di Bari. Neutrino masses, leptogenesis and dark matter. In Prospects in Neutrino Physics, 4 2019.
- [19] B. Abi et al. Measurement of the Positive Muon Anomalous Magnetic Moment to 0.46 ppm. Phys. Rev. Lett., 126(14):141801, 2021.
- [20] Peter Athron, Csaba Balázs, Douglas H. J. Jacob, Wojciech Kotlarski, Dominik Stöckinger, and Hyejung Stöckinger-Kim. New physics explanations of a_μ in light of the FNAL muon $g - 2$ measurement. JHEP, 09:080, 2021.
- [21] A. Alvarez, A. Banik, R. Cepedello, B. Herrmann, W. Porod, M. Sarazin, and M. Schnelke. Accommodating muon ($g - 2$) and leptogenesis in a scotogenic model. JHEP, 06:163, 2023.
- [22] Shintaro Eijima, Masahiro Ibe, and Kai Murai. Muon $g - 2$ and non-thermal leptogenesis in $U(1)_{L\mu-L\tau}$ model. JHEP, 05:010, 2023.
- [23] Jan Tristram Acuña, Patrick Stengel, and Piero Ullio. Minimal dark matter model for muon g -2 with scalar lepton partners up to the TeV scale. Phys. Rev. D, 105(7):075007, 2022.
- [24] Giorgio Arcadi, Álvaro S. de Jesus, Téo B. de Melo, Farinaldo S. Queiroz, and Yoxara S. Villamizar. A 2HDM for the g -2 and dark matter. Nucl. Phys. B, 982:115882, 2022.

- [25] Yang Bai and Joshua Berger. Muon $g - 2$ in Lepton Portal Dark Matter. 4 2021.
- [26] Debasish Borah, Manoranjan Dutta, Satyabrata Mahapatra, and Narendra Sahu. Lepton anomalous magnetic moment with singlet-doublet fermion dark matter in a scotogenic $U(1)L\mu-L\tau$ model. Phys. Rev. D, 105(1):015029, 2022.
- [27] Debasish Borah, Satyabrata Mahapatra, and Narendra Sahu. Singlet-doublet fermion origin of dark matter, neutrino mass and W -mass anomaly. Phys. Lett. B, 831:137196, 2022.
- [28] Ernest Ma. Verifiable radiative seesaw mechanism of neutrino mass and dark matter. Phys. Rev. D, 73:077301, 2006.
- [29] Debasish Borah, P. S. Bhupal Dev, and Abhass Kumar. TeV scale leptogenesis, inflaton dark matter and neutrino mass in a scotogenic model. Phys. Rev. D, 99(5):055012, 2019.
- [30] Devabrat Mahanta and Debasish Borah. Fermion dark matter with N_2 leptogenesis in minimal scotogenic model. JCAP, 11:021, 2019.
- [31] J. A. Casas and A. Ibarra. Oscillating neutrinos and $\mu \rightarrow e, \gamma$. Nucl. Phys. B, 618:171–204, 2001.
- [32] Takashi Toma and Avelino Vicente. Lepton Flavor Violation in the Scotogenic Model. JHEP, 01:160, 2014.
- [33] Ayres Freitas, Joseph Lykken, Stefan Kell, and Susanne Westhoff. Testing the Muon $g-2$ Anomaly at the LHC. JHEP, 05:145, 2014. [Erratum: JHEP 09, 155 (2014)].
- [34] Ethan M. Dolle and Shufang Su. The Inert Dark Matter. Phys. Rev. D, 80:055012, 2009.
- [35] Laura Lopez Honorez and Carlos E. Yaguna. The inert doublet model of dark matter revisited. JHEP, 09:046, 2010.
- [36] Adam Alloul, Neil D. Christensen, Céline Degrande, Claude Duhr, and Benjamin Fuks. FeynRules 2.0 - A complete toolbox for tree-level phenomenology. Comput. Phys. Commun., 185:2250–2300, 2014.
- [37] Neil D. Christensen and Claude Duhr. FeynRules - Feynman rules made easy. Comput. Phys. Commun., 180:1614–1641, 2009.
- [38] G. Belanger, F. Boudjema, A. Pukhov, and A. Semenov. micrOMEGAs: A Tool for dark matter studies. Nuovo Cim. C, 033N2:111–116, 2010.
- [39] G. Belanger, F. Boudjema, and A. Pukhov. micrOMEGAs : a code for the calculation of Dark Matter properties in generic models of particle interaction. In Theoretical Advanced Study Institute in Elementary Particle Physics: The Dark Secrets of the Terascale, pages 739–790, 2013.

- [40] E. Aprile et al. Excess electronic recoil events in XENON1T. Phys. Rev. D, 102(7):072004, 2020.
- [41] Yue Meng et al. Dark Matter Search Results from the PandaX-4T Commissioning Run. Phys. Rev. Lett., 127(26):261802, 2021.
- [42] E. Aprile et al. First Dark Matter Search with Nuclear Recoils from the XENONnT Experiment. Phys. Rev. Lett., 131(4):041003, 2023.
- [43] J. Aalbers et al. First Dark Matter Search Results from the LUX-ZEPLIN (LZ) Experiment. Phys. Rev. Lett., 131(4):041002, 2023.
- [44] J. Aalbers et al. DARWIN: towards the ultimate dark matter detector. JCAP, 11:017, 2016.
- [45] C. E. Aalseth et al. DarkSide-20k: A 20 tonne two-phase LAr TPC for direct dark matter detection at LNGS. Eur. Phys. J. Plus, 133:131, 2018.
- [46] D. Aristizabal Sierra, Jernej F. Kamenik, and Miha Nemevsek. Implications of Flavor Dynamics for Fermion Triplet Leptogenesis. JHEP, 10:036, 2010.
- [47] Pritam Das and Najimuddin Khan. Origin of neutrino masses, dark matter, leptogenesis, and inflation in a seesaw model with triplets. Phys. Rev. D, 107(7):075008, 2023.
- [48] Drona Vatsyayan and Srubabati Goswami. Lowering the scale of fermion triplet leptogenesis with two Higgs doublets. Phys. Rev. D, 107(3):035014, 2023.
- [49] Anirban Biswas, Mainak Chakraborty, and Sarif Khan. Reviewing the prospect of fermion triplets as dark matter and source of baryon asymmetry in non-standard cosmology. JCAP, 08:026, 2023.
- [50] Georges Aad et al. Search for type-III seesaw heavy leptons in dilepton final states in pp collisions at $\sqrt{s} = 13$ TeV with the ATLAS detector. Eur. Phys. J. C, 81(3):218, 2021.
- [51] Jeffrey A. Harvey and Michael S. Turner. Cosmological baryon and lepton number in the presence of electroweak fermion number violation. Phys. Rev. D, 42:3344–3349, 1990.